Comput. Methods Appl. Mech. Engrg. 197 (2008) 3547–3559

Contents lists available at ScienceDirect

Comput. Methods Appl. Mech. Engrg.

journal homepage: www.elsevier.com/locate/cma

Stochastic collocation and mixed finite elements for flow in porous media

Benjamin Ganis [a], Hector Klie [b,*], Mary F. Wheeler [b], Tim Wildey [b], Ivan Yotov [b], Dongxiao Zhang [c]

[a] Department of Mathematics, University of Pittsburgh, Pittsburgh, PA 15260, United States
[b] The Institute for Computational Engineering and Sciences (ICES), The University of Texas at Austin, Austin, TX 78712, United States
[c] Department of Chemical Engineering and Material Science, University of Southern California, Los Angeles, CA 90089, United States

ARTICLE INFO

Article history:
Received 15 January 2008
Received in revised form 18 March 2008
Accepted 21 March 2008
Available online 10 April 2008

Keywords:
Stochastic collocation
Mixed finite element
Stochastic partial differential equations
Flow in porous media

ABSTRACT

The aim of this paper is to quantify uncertainty of flow in porous media through stochastic modeling and computation of statistical moments. The governing equations are based on Darcy's law with stochastic permeability. Starting from a specified covariance relationship, the log permeability is decomposed using a truncated Karhunen–Loève expansion. Mixed finite element approximations are used in the spatial domain and collocation at the zeros of tensor product Hermite polynomials is used in the stochastic dimensions. Error analysis is performed and experimentally verified with numerical simulations. Computational results include incompressible and slightly compressible single and two-phase flow.

1. Introduction

In groundwater flow problems, it is physically impossible to know the exact permeability at every point in the domain. This is due to the prohibitively large scope of realistic domains, inhomogeneity in the media, and also the natural randomness occurring at very small scales. One way to cope with this difficulty is to model permeability (or porosity) as a stochastic function, determined by an underlying random field with an experimentally determined covariance structure.

The development of efficient stochastic methods that are applicable to a wide range of subsurface flow models could substantially reduce the computational costs associated with uncertainty quantification (in terms of both time and resources required). Such methods could facilitate the uncertainty analysis of complex, computationally demanding models, where traditional methods may not be feasible due to computational and time constraints. Interest in developing these methods for flow in porous media has been significant in the last years [8,27,48].

Stochastic modeling methods can be classified in three major groups: (1) sampling methods [13,24], (2) moment/perturbation methods [21,26,48,19,20] and (3) non-perturbative methods, either based on polynomial chaos expansions [16,17,42–44,18] or stochastic finite element methods [16,12,3]. In such order, we can say that these methods range from being non-intrusive to very intrusive in terms of modifying the original simulation model. The best known sampling method is Monte Carlo simulation (MCS), which involves repeated generation of random samplings (realizations) of input parameters followed by the application of the simulation model in a "black box" fashion to generate the corresponding set of stochastic responses. These responses are further analyzed to yield statistical moments or distributions. The major drawback of MCS is the high computational cost due to the need to generate valid representative statistics from a large number of realizations at a high resolution level.

Moment/perturbation and finite element stochastic methods fall into the category of non-sampling methods. These methods are suitable for systems with relatively small random inputs and outputs. However, despite the apparent accuracy and mild cost with respect to MCS, these methods also present some limitations that have prevented them from being widely used. The problem is that their semi-intrusive or fully intrusive character may greatly complicate the formulation, discretization and solution of the model equations, even in the case of linear and stationary input distributions. There is also a high computational cost associated with these methods since the number of terms needed to accurately represent the propagation of uncertainties grows significantly with respect to the degree of variability of the system. It is still not clear how these methods may be formulated in the event of high nonlinearities due to complex flow and chemical reactions over arbitrary geometries.

On the other hand, stochastic finite elements exhibit fast convergence through the use of generalized polynomial chaos representations of random processes (i.e., generalizations of the Wiener–Hermite polynomial chaos expansion to include a wider class of random processes by means of global polynomial expansions, piecewise polynomial expansions and wavelet basis expan-

* Corresponding author. Tel.: +1 512 475 8634; fax: +1 512 234 2445.
E-mail address: klie@ices.utexas.edu (H. Klie).

0045-7825/$ - see front matter © 2008 Elsevier B.V. All rights reserved.
doi:10.1016/j.cma.2008.03.025

sions; see e.g. [3,40]). However, besides their very intrusive feature, the dimensionality of the discretized stochastic finite element equations can be dramatically larger than the dimensionality of the base case deterministic model.

A very promising approach for improving the efficiency of non-sampling methods is the stochastic collocation method [2,41,45]. It combines a finite element discretization in physical space with a collocation at specially chosen points in probability space. As a result a sequence of uncoupled deterministic problems need to be solved, just like in MCS. However, the stochastic collocation method shares the approximation properties of the stochastic finite element method, making it more efficient than MCS. Choices of collocation points include tensor product of zeros of orthogonal polynomials [2,41], sparse grid approximations [15,28,30,38,41], and probabilistic collocation [25]. The last two provide approaches to reduce the number of collocation points needed to obtain a given level of approximation, leading to very efficient algorithms.

In this paper we combine mixed finite element (MFE) discretizations in physical space with stochastic collocation methods. The choice of spatial discretization is suitable for flow in porous media since it provides the solution such desired physical properties as local element-wise conservation of mass and a velocity field with continuous normal components. We study incompressible and slightly compressible single phase flow as well as two-phase flow. The paper focuses on tensor product collocation methods. Convergence analysis for the pressure and the velocity is presented for single phase incompressible and slightly compressible flow. The analysis follows the approach in [2] where standard Galerkin discretizations are studied. We show that the total error can be decomposed into the sum of deterministic and stochastic errors. Optimal convergence rates and superconvergence for the pressure are established for the deterministic error. The stochastic error converges exponentially with respect to the number of the collocation points. Numerical experiments for incompressible single phase flow as well as slightly compressible single phase and two phase flow confirm the theoretical convergence rates and demonstrate the efficiency to our approach compared to MCS. In addition, we find topological similarities between single and two-phase flow pressure trends that could be key for improving the performance of uncertainty quantification and management in complex flow systems.

The rest of the paper is organized as follows: The model problem for incompressible single phase flow is presented in Section 2. The MFE stochastic collocation method is developed in Section 3 and analyzed in Section 4. Extensions to slightly compressible single phase and two phase flow are developed in Section 5. Sections 6 and 7 contain numerical experiments for incompressible and compressible flow, respectively. Some conclusions and future directions are presented in Section 8.

2. Model problem: single phase incompressible flow

We begin with the mixed formulation of Darcy flow. Let $D \subset \mathbb{R}^d$, $d = 2, 3$ be a bounded Lipschitz domain and Ω be a stochastic event space with probability measure P. The Darcy velocity $\mathbf{u}$ and the pressure p satisfy P-almost everywhere in Ω

$$\mathbf{u} = -K(\mathbf{x}, \omega)\nabla p \quad \text{in } D, \tag{2.1}$$

$$\nabla \cdot \mathbf{u} = q \quad \text{in } D, \tag{2.2}$$

$$p = p_b \quad \text{on } \partial D. \tag{2.3}$$

For simplicity we assume Dirichlet boundary conditions. More general boundary conditions can also be considered via standard techniques. The permeability K is a diagonal tensor with uniformly positive and bounded in D elements. To simplify the presentation, we will assume that K is a scalar function. Since the permeability K is a stochastic function, p and $\mathbf{u}$ are also stochastic.

Throughout this paper the expected value of a random variable $\xi(\omega)$ with probability density function (p.d.f) $\rho(y)$ will be denoted

$$E[\xi] = \int_\Omega \xi(\omega)\,\mathrm{d}P(\omega) = \int_{\mathbb{R}} y\rho(y)\,\mathrm{d}y.$$

2.1. The Karhunen–Loève (KL) expansion

In order to guarantee positive permeability almost surely in Ω, we consider its logarithm $Y = \ln(K)$. Let the mean removed log permeability be denoted by Y', so that $Y = E[Y] + Y'$. Its covariance function $C_Y(\mathbf{x}, \bar{\mathbf{x}}) = E[Y'(\mathbf{x}, \omega)Y'(\bar{\mathbf{x}}, \omega)]$ is symmetric and positive definite, and hence can be decomposed into the series expansion

$$C_Y(\mathbf{x}, \bar{\mathbf{x}}) = \sum_{i=1}^{\infty} \lambda_i f_i(\mathbf{x}). \tag{2.4}$$

The eigenvalues λ_i and eigenfunctions f_i of this series are computed using C_Y as the kernel of the Type II Fredholm integral equation

$$\int_D C_Y(\mathbf{x}, \bar{\mathbf{x}}) f(\mathbf{x})\,\mathrm{d}\mathbf{x} = \lambda f(\bar{\mathbf{x}}). \tag{2.5}$$

The symmetry and positive definiteness of C_Y cause its eigenfunctions to be mutually orthogonal, i.e., $(f_m, f_n)_{L^2(D)} = \delta_{mn}$, and form a complete spanning set. Using this fact the Karhunen–Loève expansion of the log permeability can now be written as

$$Y(\mathbf{x}, \omega) = E[Y](\mathbf{x}) + \sum_{i=1}^{\infty} \xi_i(\omega)\sqrt{\lambda_i} f_i(\mathbf{x}), \tag{2.6}$$

where, if Y' is given by a Gaussian process, the ξ_i are mutually uncorrelated random variables with zero mean and unit variance [16].

At this point, the KL expansion is truncated after N terms, which is feasible to do as typically the λ_i decay rapidly [47]. If the expansion is truncated prematurely, the permeability may appear too smooth, so if more heterogeneity is desired then N should be increased. This truncation allows us to write $Y(\mathbf{x}, \omega) = Y(\mathbf{x}, \xi_1(\omega), \ldots, \xi_N(\omega))$. The images of the random variables $\Gamma_i = \xi_i(\Omega)$ make up a finite dimensional vector space $\Gamma = \prod_{i=1}^N \Gamma_i \subset \mathbb{R}^N$. If ρ_i corresponds to the p.d.f. of each ξ_i, then the joint p.d.f. for the random vector $(\xi_1, \ldots, \xi_N)$ is defined to be $\rho = \prod_{i=1}^N \rho_i$. Then we can write $Y(\mathbf{x}, \omega) = Y(\mathbf{x}, \mathbf{y})$, where $\mathbf{y} = (y_1, \ldots, y_N)$ and $y_i = \xi_i(\omega)$.

The numerical experiments described herein listed in Sections 6 and 7 will use the following specific covariance function (in 2-D) originally taken from [47], in which λ_i and $f_i(\mathbf{x})$ can be found analytically

$$C_Y(\mathbf{x}, \bar{\mathbf{x}}) = \sigma_Y^2 \exp\left[\frac{-|x_1 - \bar{x}_1|}{\eta_1} - \frac{|x_2 - \bar{x}_2|}{\eta_2}\right]. \tag{2.7}$$

Here σ_Y and η_i denote variance and correlation length in the ith spatial dimension, respectively. This covariance kernel is separable, so Eq. (2.5) can be solved in each dimension individually, and then its eigenvalues and eigenfunctions can be assembled by multiplication. These eigenvalues will decay at a rate asymptotic to $O(1/N^2)$ and for this particular case can be computed analytically.

When the exact eigenvalues and eigenfunctions of the covariance function C_Y can be found, the KL expansion is the most efficient method for representing a random field. However, in most cases, closed-form eigenfunctions and eigenvalues are not readily available and numerical procedures need be performed for solving the integral Eq. (2.5). Efficient methods for numerically computing the KL expansion are reported in [37].

2.2. Variational formulation

Appealing to the Doob–Dynkn Lemma [31], the p.d.f. for the permeability K carries through to the solution of (2.1)–(2.3), so that $(\mathbf{u}, p)$ has the form

$$\mathbf{u}(\mathbf{x},\omega) = \mathbf{u}(\mathbf{x},\xi_1(\omega),\ldots,\xi_N(\omega)) = \mathbf{u}(\mathbf{x},y_1,\ldots,y_N) \quad \text{and}$$
$$p(\mathbf{x},\omega) = p(\mathbf{x},\xi_1(\omega),\ldots,\xi_N(\omega)) = p(\mathbf{x},y_1,\ldots,y_N).$$

Since we will be computing statistical moments of the stochastic solution to the mixed formulation of Darcy's Law, this naturally leads to introduce the spaces $\mathbf{V}(D,\Gamma) = H(\mathrm{div};D)\otimes L^2(\Gamma)$ and $W(D,\Gamma) = L^2(D)\otimes L^2(\Gamma)$ with norms

$$\|\mathbf{v}\|_V^2 = \int_\Gamma \rho(\mathbf{y}) \int_D (\mathbf{v}\cdot\mathbf{v} + (\nabla\cdot\mathbf{v})^2)\,d\mathbf{x}\,d\mathbf{y} = E[\|\mathbf{v}\|^2_{H(\mathrm{div};D)}] \quad \text{and}$$
$$\|w\|_W^2 = \int_\Gamma \rho(\mathbf{y}) \int_D w^2\,d\mathbf{x}\,d\mathbf{y} = E[\|w\|^2_{L^2(D)}].$$

The usual multiplication by a test function $\mathbf{v}\in\mathbf{V}(D,\Gamma)$ and $w\in W(D,\Gamma)$ and subsequent application of Green's Theorem in the system (2.1)–(2.3) leads to the weak formulation. That is, to find $\mathbf{u}(\mathbf{x},\omega)\in\mathbf{V}(D,\Gamma), p(\mathbf{x},\omega)\in W(D,\Gamma)$ such that

$$\int_\Gamma (K^{-1}\mathbf{u},\mathbf{v})_{L^2(D)}\rho(\mathbf{y})\,d\mathbf{y} = \int_\Gamma ((p,\nabla\cdot\mathbf{v})_{L^2(D)} - \langle p_b,\mathbf{v}\cdot\mathbf{n}\rangle_{L^2(\partial D)})\rho(\mathbf{y})\,d\mathbf{y}, \quad \forall\mathbf{v}\in\mathbf{V}(D,\Gamma), \tag{2.8}$$

$$\int_\Gamma (\nabla\cdot\mathbf{u},w)_{L^2(D)}\rho(\mathbf{y})\,d\mathbf{y} = \int_\Gamma (q,w)_{L^2(D)}\rho(\mathbf{y})\,d\mathbf{y}, \quad \forall w\in W(D,\Gamma), \tag{2.9}$$

where $\mathbf{n}$ is the outward normal to ∂D.

3. Stochastic collocation for mixed finite element methods

After expressing the log permeability as a truncated KL expansion, the problem has now been reformulated in the finite dimensional space $D\otimes\Gamma\in\mathbb{R}^{d+N}$. At this point, there are several ways in which to discretize the problem. The Stochastic Finite Element Method (SFEM) [12] considers solving the problem using full $d+N$ dimensional finite elements. This method essentially attempts to tackle a single and coupled high dimensional problem at one fell swoop. The resulting system is significantly large, difficult to set up, and the solution algorithm does not easily lend itself to parallelization.

A less intrusive approach is to use d-dimensional finite elements in the spatial domain D, and to sample the stochastic space Γ only at certain points. By a simple Monte Carlo approach for instance, we may choose M random stochastic points, and a deterministic FEM problem may then be solved in physical space at each realization. Finally, these solutions may then be averaged together in order to compute the various statistical moments of the stochastic solution. The advantage of this method is that the deterministic FEM problems are completely uncoupled, and may be solved in parallel. The disadvantage of this method is that the convergence rate is slow, e.g., $\|p - p^M_{\mathrm{MC}}\|_W = \mathrm{O}(1/\sqrt{M})$.

The Stochastic Collocation Method improves upon the Monte Carlo approach by sampling at specially chosen collocation points in order to form a polynomial interpolant in the stochastic space. Different varieties of stochastic collocation arise by considering different sets of collocation points. The simplest approach is a full tensor product grid of collocation points. This will be the method that is considered henceforth.

It should be noted that full tensor product grids of collocation points suffer from the so-called" curse of dimensionality". Increasing the number of terms in the truncated KL expansion (2.6) increases the number of stochastic dimensions in Γ which exponentially increases the number of points in a full tensor product grid. To cope with this problem, more advanced collocation techniques are possible such as the so called probabilistic collocation method (see e.g. [25]) and the Smolyak sparse grids (see e.g. [30,45]) but will not be considered in this paper.

3.1. Mixed finite element semidiscrete formulation

Let $\mathscr{T}_h$ be a shape-regular affine finite element partition of the spatial domain D [10]. A mixed finite element discretization $\mathbf{V}_h(D)\times W_h(D)\subset H(\mathrm{div},D)\times L^2(D)$ is chosen to satisfy a discrete *inf–sup* condition. The semidiscrete formulation will be to find $\mathbf{u}_h:\Gamma\to\mathbf{V}_h(D)$ and $p_h:\Gamma\to W_h(D)$ such that for a.e. $\mathbf{y}\in\Gamma$,

$$(K^{-1}\mathbf{u}_h,\mathbf{v}_h)_{L^2(D)} = (p_h,\nabla\cdot\mathbf{v}_h)_{L^2(D)} - \langle p_b,\mathbf{v}_h\cdot\mathbf{n}\rangle_{L^2(\partial D)}, \quad \forall\mathbf{v}_h\in\mathbf{V}_h(D), \tag{3.1}$$

$$(\nabla\cdot\mathbf{u}_h,w_h)_{L^2(D)} = (q,w_h)_{L^2(D)}, \quad \forall w_h\in W_h(D). \tag{3.2}$$

By the general saddle point problem theory [7], a solution to this problem exists and it is unique.

Any of the usual mixed finite element spaces may be considered, including the RTN spaces [36,29], BDM spaces [6], BDFM spaces [5], BDDF spaces [4], or CD spaces [9]. On each element E in the mesh, assume that the velocity space $\mathbf{V}_h(E)$ contains $(\mathbb{P}_r(E))^d$, $r\geqslant 0$, with normal components on each edge (face) in $\mathbb{P}_r(\gamma)$, and that the pressure space $W_h(E)$ contains $\mathbb{P}_s(E)$. In all of the above mixed FEM spaces, $s=r$ or $s=r-1$ when $r\geqslant 1$. In the numerical experiments in Section 6, the lowest order Raviart–Thomas RT_0 spaces will be used on a uniform mesh of rectangular elements in 2-D.

3.2. Stochastic collocation and fully discrete formulation

Let $\{\mathbf{y}_k\}$, $k=1,\ldots,M_m$ be a collection of points which form a Haar set in Γ. Then these points will generate a unique N dimensional polynomial interpolant I_m of total degree m across the stochastic space. The fully discrete solution is define to be

$$\mathbf{u}_{h,m}(\mathbf{x},\mathbf{y}) = I_m\mathbf{u}_h(\mathbf{x},\mathbf{y}), \qquad p_{h,m}(\mathbf{x},\mathbf{y}) = I_m p_h(\mathbf{x},\mathbf{y}).$$

Let $(\mathbf{u}_h(\mathbf{x},\mathbf{y}_k), p_h(\mathbf{x},\mathbf{y}_k))$ solve (3.1) and (3.2) for $k=1,\ldots,M_m$. Then the fully discrete solution has the Lagrange representation:

$$\mathbf{u}_{h,m}(\mathbf{x},\mathbf{y}) = \sum_{k=1}^{M_m}\mathbf{u}_h(\mathbf{x},\mathbf{y}_\mathbf{k})l_k(\mathbf{y}), \tag{3.3}$$

$$p_{h,m}(\mathbf{x},\mathbf{y}) = \sum_{k=1}^{M_m}p_h(\mathbf{x},\mathbf{y}_\mathbf{k})l_k(\mathbf{y}), \tag{3.4}$$

where $\{l_k\}$ is the Lagrange basis $l_k(y_j)=\delta_{kj}$. As previously described, to compute each $\mathbf{u}_{h,m}$ and $p_{h,m}$ it is necessary to solve M_m uncoupled deterministic problems.

In practice, this Lagrange representation is not actually assembled, since the end goal will be the computation of the stochastic solution's statistical moments such as expectation and variance. After solving each deterministic problem at a collocation point, a running total is tabulated in a weighted sum, e.g.,

$$E[p_{h,m}](\mathbf{x}) = \int_\Gamma p_{h,m}(\mathbf{x},\mathbf{y})\rho(\mathbf{y})\,d\mathbf{y} = \int_\Gamma I_m p_h(\mathbf{x},\mathbf{y})\rho(\mathbf{y})\,d\mathbf{y}$$
$$= \int_\Gamma \sum_{k=1}^{M_m} p_h(\mathbf{x},\mathbf{y}_\mathbf{k})l_k(\mathbf{y})\rho(\mathbf{y})\,d\mathbf{y} = \sum_{k=1}^{M_m} w_k p_h(\mathbf{x},\mathbf{y}_\mathbf{k}),$$

where the weights $w_k = \int_\Gamma l_k(\mathbf{y})\rho(\mathbf{y})\,d\mathbf{y}$.

3.3. Tensor product collocation

For stochastic collocation using a full tensor product grid, assume that we wish to obtain accuracy up to polynomial of degree m_i in the ith component of Γ. This will require m_i+1 points in the ith direction. Let $m=(m_1,\dots,m_N)$ and define the space $P_m(\Gamma)=P_{m_1}(\Gamma_1)\otimes\cdots\otimes P_{m_N}(\Gamma_N)$. Then the total number of collocation points needed will be $M=\dim P_m(\Gamma)=\prod_{i=1}^N(m_i+1)$.

The one dimensional collocation points on the component Γ_i will be the m_i+1 zeros of the orthogonal polynomial q_{m_i+1} with respect to the inner-product $(u,v)_{\rho_i}=\int_{\Gamma_i}u(y)v(y)\rho_i(y)\,dy$. Let $I^i_{m_i}\in P_{m_i}(\Gamma_i)$ be the one-dimensional interpolant:

$$I^i_{m_i}u(\cdot,y_{i,k})=u(\cdot,y_{i,k}),\quad k=1,\dots,m_i+1.$$

Since the choice was made in Section 2.1 to use the particular covariance function (2.7), with its KL expansion consisting of $N(0,1)$ Gaussian distributed random variables, we have $\rho_i=\frac{1}{\sqrt{2\pi}}e^{-y_i^2/2}$ and $\Gamma_i=\mathbb{R}$. The corresponding orthogonal polynomials under this inner product will be the global Hermite polynomials

$$H_{m_i}(y)=m_i!\sum_{j=0}^{\lfloor m_i/2\rfloor}(-1)^j\frac{(2y)^{m_i-2j}}{j!(m_i-2j)!},$$

and their roots can be found tabulated in [1] or computed with a symbolic manipulation software package.

4. Error analysis for single phase incompressible flow

The error between the true stochastic velocity $\mathbf{u}$ and the approximate fully discrete velocity $\mathbf{u}_{h,m}$ may be decomposed by adding and subtracting the semidiscrete velocity $\mathbf{u}_h$

$$\begin{aligned}\|\mathbf{u}-\mathbf{u}_{h,m}\|_V&\leqslant\|\mathbf{u}-\mathbf{u}_h\|_V+\|\mathbf{u}_h-\mathbf{u}_{h,m}\|_V\\&=\|\mathbf{u}-\mathbf{u}_h\|_V+\|\mathbf{u}_h-I_m\mathbf{u}_h\|_V.\end{aligned}$$

A similar decomposition holds for $\|p-p_{h,m}\|_W$. An *a priori* bound on the first term follows, assuming enough smoothness of the solution, from standard deterministic mixed FEM error analysis [7]

$$\begin{aligned}\|\mathbf{u}-\mathbf{u}_h\|_V^2+\|p-p_h\|_W^2&=\int_\Gamma\Big(\|\mathbf{u}-\mathbf{u}_h\|^2_{H(\mathrm{div};D)}+\|p-p_h\|^2_{L^2(D)}\Big)\rho(\mathbf{y})\,d\mathbf{y}\\&\leqslant C\int_\Gamma\Big(h^{2r+2}\|\mathbf{u}\|^2_{H^{r+1}(D)}+h^{2s+2}\|\nabla\cdot\mathbf{u}\|^2_{H^{s+1}(D)}\\&\quad+h^{2s+2}\|p\|^2_{H^{s+1}(D)}\Big)\rho(\mathbf{y})\,d\mathbf{y}\\&=C\Big(h^{2r+2}\|\mathbf{u}\|^2_{H^{r+1}(D)\otimes L^2(\Gamma)}\\&\quad+h^{2s+2}\|\nabla\cdot\mathbf{u}\|^2_{H^{s+1}(D)\otimes L^2(\Gamma)}\\&\quad+h^{2s+2}\|p\|^2_{H^{s+1}(D)\otimes L^2(\Gamma)}\Big).\end{aligned}$$

For the second term, an interpolation bound on Γ has recently been found in [2] to be

$$\|\mathbf{u}_h-I_m\mathbf{u}_h\|_V+\|p_h-I_mp_h\|_W\leqslant C\sum_{i=1}^N e^{-c_i\sqrt{m_i}},$$

where $c_i>0$ are defined in [2]. In particular, it is shown in [2] that if K is smooth enough in Γ, then the solution admits an analytic extension in a region of the complex plane containing Γ_i for $i=1,\dots,N$, and that c_i depends on the distance between Γ_i and the nearest singularity in the complex plane. The KL expansion (2.6) satisfies the smoothness assumption in [2]. As a result we have the following theorem.

Theorem 4.1. *Assume that* $\mathbf{u}\in H^{r+1}(D)\otimes L^2(\Gamma)$, $\nabla\cdot\mathbf{u}\in H^{s+1}(D)\otimes L^2(\Gamma)$, *and* $p\in H^{s+1}(D)\otimes L^2(\Gamma)$. *Then there exists a constant* C *independent of* h *and* M *such that*

$$\|\mathbf{u}-\mathbf{u}_{h,m}\|_V+\|p-p_{h,m}\|_W\leqslant C\left(h^{r+1}+h^{s+1}+\sum_{i=1}^N e^{-c_i\sqrt{m_i}}\right).$$

We next establish a superconvergence bound for the pressure. For $\varphi\in L^2(D)$, denote with $\hat\varphi$ its L^2-projection in W_h satisfying

$$(\varphi-\hat\varphi,w_h)_{L^2(D)}=0\quad\forall\,w_h\in W_h,\tag{4.1}$$

$$\|\varphi-\hat\varphi\|_{L^2(D)}\leqslant Ch^l\|\varphi\|_{H^l(D)},\quad 0\leqslant l\leqslant s+1.\tag{4.2}$$

Let $\Pi:(H^1(D))^d\to\mathbf{V}_h(D)$ be the mixed finite element projection operator satisfying

$$(\nabla\cdot(\mathbf{u}-\Pi\mathbf{u}),w_h)_{L^2(D)}=0\quad\forall w_h\in W_h,\tag{4.3}$$

$$\|\mathbf{u}-\Pi\mathbf{u}\|_{(L^2(D))^d}\leqslant Ch^l\|\mathbf{u}\|_{(H^l(D))^d},\quad 1\leqslant l\leqslant r+1.\tag{4.4}$$

Theorem 4.2. *Assume that problem (2.1)–(2.3) is* H^2*-elliptic regular. Under the assumptions of Theorem 4.1, there exists a constant* C *independent of* h *and* M *such that*

$$\|\hat p-p_{h,m}\|_W\leqslant C(h\|\mathbf{u}-\mathbf{u}_h\|_V+\|p_h-I_mp_h\|_W).$$

Proof. The proof is based on a duality argument. Taking $\mathbf{v}=\mathbf{v}_h$ and $w=w_h$ in the weak formulation (2.8)–(2.9) and subtracting the semidiscrete formulation (3.1)–(3.2) gives the error equations for a.e. $\mathbf{y}\in\Gamma$

$$(K^{-1}(\mathbf{u}-\mathbf{u}_h),\mathbf{v}_h)_{L^2(D)}=(\hat p-p_h,\nabla\cdot\mathbf{v}_h)_{L^2(D)}\quad\forall\mathbf{v}_h\in\mathbf{V}_h(D),\tag{4.5}$$

$$(\nabla\cdot(\mathbf{u}-\mathbf{u}_h),w_h)_{L^2(D)}=0\quad\forall w_h\in W_h(D).\tag{4.6}$$

Now consider the following auxiliary problem in mixed form:

$$\begin{aligned}&\boldsymbol{\psi}(\cdot,\mathbf{y})=-K(\cdot,\mathbf{y})\nabla\varphi(\cdot,\mathbf{y})\quad\text{in } D,\\&\nabla\cdot\boldsymbol{\psi}(\cdot,\mathbf{y})=\hat p-p_{h,m}\quad\text{in } D,\\&\varphi(\cdot,\mathbf{y})=0\quad\text{on }\partial D.\end{aligned}$$

The elliptic regularity implies

$$\|\varphi(\cdot,\mathbf{y})\|_{H^2(D)}\leqslant C\|\hat p-p_{h,m}\|_{L^2(D)}.\tag{4.7}$$

Therefore,

$$\begin{aligned}\|\hat p-p_{h,m}\|_W^2&=\int_\Gamma(\hat p-p_{h,m},\hat p-p_{h,m})_{L^2(D)}\rho(\mathbf{y})\,d\mathbf{y}\\&=\int_\Gamma(\nabla\cdot\boldsymbol{\psi},\hat p-p_{h,m})_{L^2(D)}\rho(\mathbf{y})\,d\mathbf{y}\\&=\int_\Gamma((\nabla\cdot\boldsymbol{\psi},\hat p-p_h)_{L^2(D)}+(\nabla\cdot\boldsymbol{\psi},p_h-I_mp_h)_{L^2(D)})\rho(\mathbf{y})\,d\mathbf{y}\\&=I+II.\end{aligned}$$

Applying the Cauchy–Schwarz inequality, we have

$$\begin{aligned}|II|&\leqslant\left(\int_\Gamma\|\nabla\cdot\boldsymbol{\psi}\|^2_{L^2(D)}\rho(\mathbf{y})\,d\mathbf{y}\right)^{1/2}\left(\int_\Gamma\|p_h-I_mp_h\|^2_{L^2(D)}\rho(\mathbf{y})\,d\mathbf{y}\right)^{1/2}\\&=\left(\int_\Gamma\|\hat p-p_{h,m}\|^2_{L^2(D)}\rho(\mathbf{y})\,d\mathbf{y}\right)^{1/2}\|p_h-I_mp_h\|_W\\&=\|\hat p-p_{h,m}\|_W\|p_h-I_mp_h\|_W.\end{aligned}$$

Using (4.3) and (4.5) with $\mathbf{v}_h=\Pi\boldsymbol{\psi}$,

$$\begin{aligned}I&=\int_\Gamma(K^{-1}(\mathbf{u}-\mathbf{u}_h),\Pi\boldsymbol{\psi})_{L^2(D)}\rho(\mathbf{y})\,d\mathbf{y}\\&=\int_\Gamma((K^{-1}(\mathbf{u}-\mathbf{u}_h),\Pi\boldsymbol{\psi}-\boldsymbol{\psi})_{L^2(D)}-(\mathbf{u}-\mathbf{u}_h,\nabla\varphi)_{L^2(D)})\rho(\mathbf{y})\,d\mathbf{y}\\&=I_1+I_2.\end{aligned}$$

The Cauchy–Schwarz inequality, (4.4), and (4.7) imply

$$|I_1| \leqslant C\left(\int_\Gamma \|\mathbf{u}-\mathbf{u}_h\|^2_{L^2(D)}\rho(\mathbf{y})\,d\mathbf{y}\right)^{1/2}\left(\int_\Gamma \|\Pi\psi-\psi\|^2_{L^2(D)}\rho(\mathbf{y})\,d\mathbf{y}\right)^{1/2}$$
$$\leqslant C\|\mathbf{u}-\mathbf{u}_h\|_V h\left(\int_\Gamma \|\psi\|^2_{(H^1(D))^d}\rho(\mathbf{y})\,d\mathbf{y}\right)^{1/2}$$
$$\leqslant Ch\|\mathbf{u}-\mathbf{u}_h\|_V\|\hat{p}-p_{h,m}\|_W.$$

Using (4.6), (4.1), and (4.7), we have

$$|I_2| = \left|\int_\Gamma (\nabla\cdot(\mathbf{u}-\mathbf{u}_h),\varphi-w_h)_{L^2(D)}\rho(\mathbf{y})\,d\mathbf{y}\right|$$
$$\leqslant C\|\mathbf{u}-\mathbf{u}_h\|_V h\|\hat{p}-p_{h,m}\|_W.$$

A combination of the above estimates completes the proof of the theorem. □

Corollary 4.3. *Under the assumptions of Theorem 4.2, there exists a constant C independent of h and M such that*

$$\|\hat{p}-p_{h,m}\|_W \leqslant C\left(h^{r+2}+h^{s+2}+\sum_{i=1}^{N} e^{-c_i\sqrt{m_i}}\right).$$

5. Slightly compressible single and two-phase flow

In this section, we describe the extension of the stochastic methods discussed in previous sections to the nonlinear conservation equations governing multiphase flow in porous media. Previous theoretical results are extended to slightly compressible flows. For the the two-phase case only numerical results are reported since few *a priori* estimates are known.

5.1. Two-phase flow

In the case of slightly compressible flow, the porosity ϕ and permeability tensor K are spatially varying and constant in time reservoir data. We remark that in the general case, both porosity and permeability may be stochastic random variables in space and mutually correlated. For simplicity, we consider only the permeability to be stochastic. Other rock properties involve relative permeability and capillary pressure relationships which are given functions of saturations and possible also of position in the case of different rock types. The well injection and production rates are defined using the Peaceman well model [34] extended to multiphase and multicomponent flow, and they describe typical well conditions for pressure or rate specified wells.

Let the lower case scripts w and o denote the water and oil phase respectively. The corresponding phase saturations are denoted by S_w and S_o, the phase pressures by p_w and p_o, and the well injection/production rates by q_w and q_o.

Consider the two-phase immiscible slightly compressible oil-water flow model in which the densities of oil and water are given by the equation of state,

$$\rho_n = \rho_n^{\mathrm{ref}} e^{c_n(p_n-p_n^{\mathrm{ref}})}, \tag{5.1}$$

where ρ_n^{ref} is the reference density, p_n^{ref} is the reference pressure, and c_n is the compressibility for $n = w, o$. The mass conservation equation and Darcy's law are

$$\mathbf{u}_n = -\frac{K(\mathbf{x},\omega)}{\mu_n}\rho_n k_n(\nabla p-\rho_n G\nabla\mathscr{D}) \quad \text{in } D\times J, \tag{5.2}$$
$$\frac{\partial}{\partial t}(\phi S_n\rho_n)+\nabla\cdot\mathbf{u}_n = q_n \quad \text{in } D\times J, \tag{5.3}$$
$$p_n = p_{n,b} \quad \text{on } \partial D\times J, \tag{5.4}$$
$$p_n = p_{n,0} \quad \text{in } D\times\{0\}, \tag{5.5}$$

subject to the constitutive constraints

$$S_o+S_w = 1,$$
$$p_c(S_w) = p_o-p_w,$$

where μ_n is the density, G the magnitude of the gravitational acceleration, $\mathscr{D}$ the depth, and $J=[0,T]$.

5.2. Error analysis for single phase slightly compressible flow

In the case $S_o = 0$, Eqs. (5.2)–(5.5) reduce to

$$\mathbf{u} = -\frac{K(\mathbf{x},\omega)}{\mu}\rho_w(\nabla p-\rho_w G\nabla\mathscr{D}) \quad \text{in } D\times J, \tag{5.6}$$
$$\frac{\partial}{\partial t}(\phi\rho_w)+\nabla\cdot\mathbf{u} = q \quad \text{in } D\times J, \tag{5.7}$$
$$p = p_b \quad \text{on } \partial D\times J, \tag{5.8}$$
$$p = p_0 \quad \text{in } D\times\{0\}. \tag{5.9}$$

We retain the subscript w on the density to distinguish this quantity from the probability density function. We make the following assumptions on the data. There is a positive constant α such that

(A1) $\phi\in L^\infty(D)$ and $\frac{1}{\alpha}\leqslant\phi(\mathbf{x})\leqslant\alpha$,
(A2) $\rho_w\in W^{2,\infty}(\mathbb{R})$ and $\frac{1}{\alpha}\leqslant\rho_w,\rho_w',\rho_w''\leqslant\alpha$.

The semidiscrete weak formulation seeks $\mathbf{u}_h : \Gamma\times J\to\mathbf{V}_h(D)$ and $p_h:\Gamma\times J\to W_h(D)$ such that for a.e. $\mathbf{y}\in\Gamma$,

$$\left(\left(\frac{K\rho_{w,h}}{\mu}\right)^{-1}\mathbf{u}_h,\mathbf{v}_h\right)_{L^2(D)} = (p_h,\nabla\cdot\mathbf{v}_h)_{L^2(D)}-(\rho_{w,h}G\nabla\mathscr{D},\mathbf{v}_h)_{L^2(D)}$$
$$-\langle p_b,\mathbf{v}_h\cdot\mathbf{n}\rangle_{L^2(\partial D)}, \tag{5.10}$$
$$\left(\frac{\partial}{\partial t}(\phi\rho_{w,h}),w_h\right)_{L^2(D)}+(\nabla\cdot\mathbf{u}_h,w_h)_{L^2(D)} = (q,w_h)_{L^2(D)}, \tag{5.11}$$

for all $\mathbf{v}_h\in\mathbf{V}_h(D)$ and $w_h\in W_h(D)$ with the initial condition $p_h(0)=\dot{p_0}$, the $L^2(D)$ projection of p_0 onto $W_h(D)$. To discretize in stochastic space, we select a tensor product set of collocation points based on the roots of orthogonal Hermite polynomials, and use the Lagrange representations (3.3) and (3.4) for the velocity and pressure respectively.

Define $\mathbf{V}_J = L^2(\Gamma)\otimes L^p(J)\otimes H(\mathrm{div};D)$, and $W_J = L^2(\Gamma)\otimes L^p(J)\otimes L^2(D)$, with the norms

$$\|\mathbf{v}\|^2_{V_J} = \int_\Gamma \rho(\mathbf{y})\left(\int_J \|\mathbf{v}\|^p_{H(\mathrm{div};D)}dt\right)^{1/p}d\mathbf{y},$$
$$\|w\|^2_{W_J} = \int_\Gamma \rho(\mathbf{y})\left(\int_J \|w\|^p_{L^2(D)}dt\right)^{1/p}d\mathbf{y},$$

where if $p=\infty$, the integral is replaced by the essential supremum.

As before, we add and subtract the semidiscrete velocity, splitting the error into

$$\|\mathbf{u}-\mathbf{u}_{h,m}\|_{V_J} = \|\mathbf{u}-\mathbf{u}_h\|_{V_J}+\|\mathbf{u}-I_m\mathbf{u}_h\|_{V_J},$$

which represents a deterministic discretization error and a stochastic error. Similar decomposition holds for $\|p-p_{h,m}\|_{W_J}$. Using the deterministic error bounds [22,23,33]

$$\|\mathbf{u}-\mathbf{u}_h\|_{H(\mathrm{div};D)\otimes L^p(J)}+\|p-p_h\|_{L^2(D)\otimes L^p(J)}$$
$$\leqslant C\Big(h^{r+1}\|\mathbf{u}\|_{H^{r+1}(D)\otimes L^p(J)}+h^{s+1}\|\nabla\cdot\mathbf{u}\|_{H^{s+1}(D)\otimes L^p(J)}$$
$$+h^{s+1}\|p\|_{H^{s+1}(D)\otimes L^p(J)}\Big),$$

and the argument for the proof of Theorem 4.1, we obtain the following result.

Theorem 5.1. *Assume that* $\mathbf{u}\in H^{r+1}(D)\otimes L^p(J)\otimes L^2(\Gamma)$, $\nabla\cdot\mathbf{u}\in H^{s+1}(D)\otimes L^p(J)\otimes L^2(\Gamma)$, *and* $p\in H^{s+1}(D)\otimes L^p(J)\otimes L^2(\Gamma)$. *Then there exists a constant C independent of h and M such that*

$$\|\mathbf{u}-\mathbf{u}_{h,m}\|_{V_J}+\|p-p_{h,m}\|_{W_J}\leqslant C\left(h^{r+1}+h^{s+1}+\sum_{i=1}^{N}e^{-c_i\sqrt{m_i}}\right).$$

6. Numerical experiments for single phase incompressible flow

The numerical experiments in this section were programmed using the parallel mixed finite element software package PARCEL [11], which is written in FORTRAN and parallelized using the Message Passing Interface (MPI) Library. The MFE space is taken to be the lowest order Raviart–Thomas RT_0 space on a uniform mesh of rectangular 2-D elements, which is also equivalent to a cell-centered finite difference approximation. This code divides the problem into 4 non-overlapping subdomains and the problem is reformulated in terms of new variables along the subdomain interfaces. This reduced interface problem is solved using a conjugate gradient iteration with a balancing domain decomposition preconditioner.

The covariance function (2.7) was used to generate the KL expansion of an isotropic permeability field, as given in [47]. The algorithm starts by pre-computing and storing the eigenvalues and cell-centered eigenfunction values for the KL expansion. Implementation of the stochastic collocation method was achieved by adding a loop around the deterministic solver and supplying it with permeability realizations at each stochastic collocation point. The solutions for both stochastic pressure and velocity are then averaged together using the collocation weights in order to compute their expectation and variance.

All numerical experiments are solved on the square domain $[0,1]\times[0,1]$. Each use the same KL expansion for mean removed log permeability Y' with variance $\sigma_Y = 1$, correlation lengths $\eta_1 = 0.20$, $\eta_2 = 0.125$, and are truncated after $N = 6$ terms.

In the numerical error studies, the reported pressure error is the discrete L^2 error computed at the cell centers. The velocity error is the discrete L^2 error computed at the midpoints of the edges. The flux error is the discrete L^2 error of the flux through the subdomain interfaces computed at the midpoints of the edges. The stochastic convergence is computed on a fixed 80×80 spatial mesh. The expected solutions on stochastic tensor product grids made up of 2,3,4 collocation points in 6 stochastic dimensions are compared to the mean solution using 5 collocation points. The deterministic convergence is computed using a fixed stochastic tensor product grid of with 4 collocation points in 6 stochastic dimensions. The spatial mesh is refined from a 10×10 grid to an 80×80 grid, and error is computed against the numerical solution on a 160×160 grid.

We consider three cases:

- Problem A: Flow from left to right,
- Problem B: Quarter five-spot well distribution, and
- Problem C: Discontinuous permeability field.

6.1. Problem A: flow from left to right test

Problem A has Dirichlet boundary conditions $p = 1$ on $\{x_1 = 0\}$, $p = 0$ on $\{x_1 = 1\}$ and Neumann boundary conditions $\mathbf{u}\cdot\mathbf{n} = 0$ specified on both $\{x_2 = 0\}$, $\{x_2 = 1\}$. The source function is $q = 0$. The log permeability Y has zero mean.

Fig. 1 shows a typical Monte Carlo realization of the isotropic permeability field, and its corresponding solution. Figs. 2 and 3 show the expectation and variance of the stochastic solution. The pressure variance is largest in a vertical strip in the middle of the domain, away from the Dirichlet boundary edges. The velocity variance is smallest along the Neumann edges and it is affected by the direction of the flow. Table 1 shows the stochastic convergence. We note that exponential convergence is observed for the stochastic error. Table 2 shows the deterministic convergence. The num-

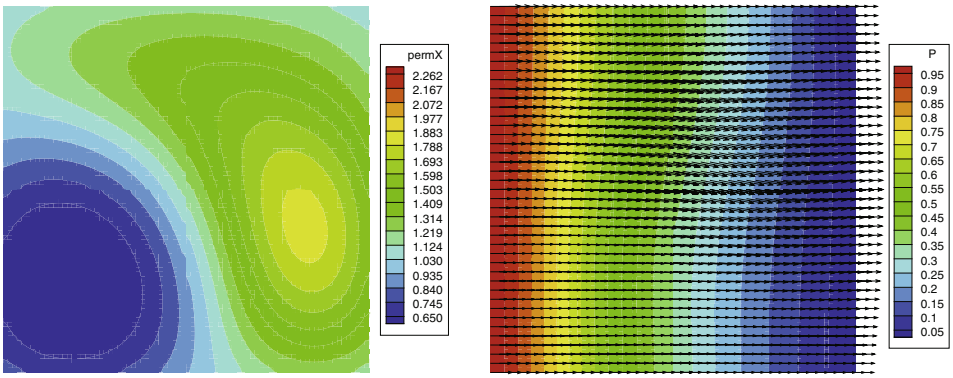

Fig. 1. A Monte Carlo realization of the permeability field (left) and its corresponding solution (right) to problem A with six terms in KL expansion.

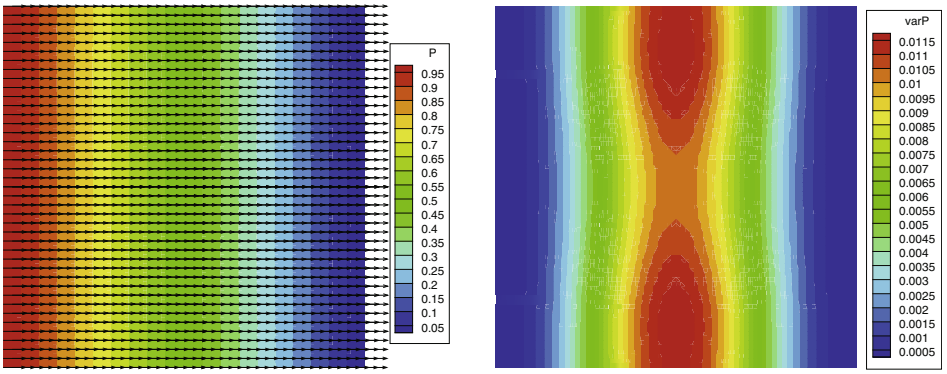

Fig. 2. Expectation of solution (left), and variance of the pressure (right) to problem A with 4^6 collocation points.

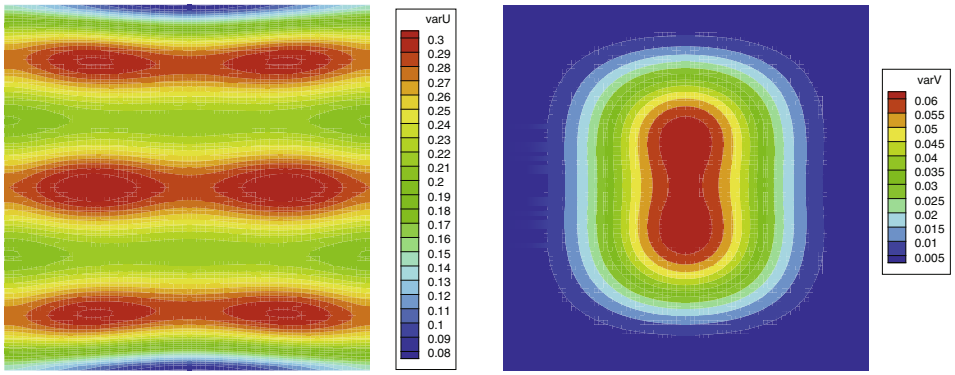

Fig. 3. Variance of the x-velocity component (left), and variance of the y-velocity component (right) to problem A with 4^6 collocation points.

Table 1
Stochastic convergence results for problem A

Coll. points	Flux L2 error	Pressure L2 error	Velocity L2 error
2^6	2.34725998E−03	1.88268447E−05	1.63386987E−03
3^6	5.62408269E−05	1.20132144E−06	3.86677083E−05
4^6	3.85038674E−06	1.00645052E−07	2.62419902E−06

bers in parenthesis are the ratios between the errors on successive levels of refinement. Superconvergence of the deterministic error is observed for both the pressure and the velocity, confirming the theory.

6.2. Problem B: quarter five-spot test

Problem B has no-flow boundary conditions $\mathbf{u} \cdot \mathbf{n} = 0$ on ∂D. The spatial mesh is made up of 80×80 elements. The source function has a source $q = 100$ in the upper left element and a sink $q = -100$ in the lower right element, and is everywhere else $q = 0$. The log permeability Y has zero mean.

Figs. 4 and 5 show the expectation and variance of the stochastic solution to problem B. The pressure variance is largest at the wells and so is the velocity variance. However, the velocity variance is also affected by the no flow boundary conditions. Table 3 shows the stochastic convergence. We again observe exponential convergence.

6.3. Problem C: discontinuous permeability test

Problem C has the same boundary conditions and source function as problem A. The log permeability Y has a mean of 4.6 in lower-left and upper-right subdomains, and zero mean in upper-left and lower-right subdomains.

Figs. 6 and 7 show the expectation and variance of the stochastic solution to problem C. The pressure variance is largest in the regions where the pressure changes the most. The velocity variance is largest at the cross-point, where the solution is singular and the true velocity is infinite. Table 4 shows the stochastic convergence. Despite the singularity in physical space, the solution preserves it smoothness in stochastic space, and exponential convergence is observed. Table 5 shows the deterministic convergence. Due to the singularity at the cross-point, the convergence rates have deteriorated, but appear to be approaching first order for both the pressure and velocity.

Table 2
Deterministic convergence results for problem A

Grid	Flux L2 error	Pressure L2 error	Velocity L2 error
10×10	9.22149E−04	1.11495E−04	9.26733E−04
20×20	2.33581E−04 (3.9479)	2.73432E−05 (4.0776)	2.46538E−04 (3.7590)
40×40	5.59873E−05 (4.1720)	6.50603E−06 (4.2028)	5.99880E−05 (4.1098)
80×80	1.17766E−05 (4.7541)	1.30309E−06 (4.9927)	1.21597E−05 (4.9333)

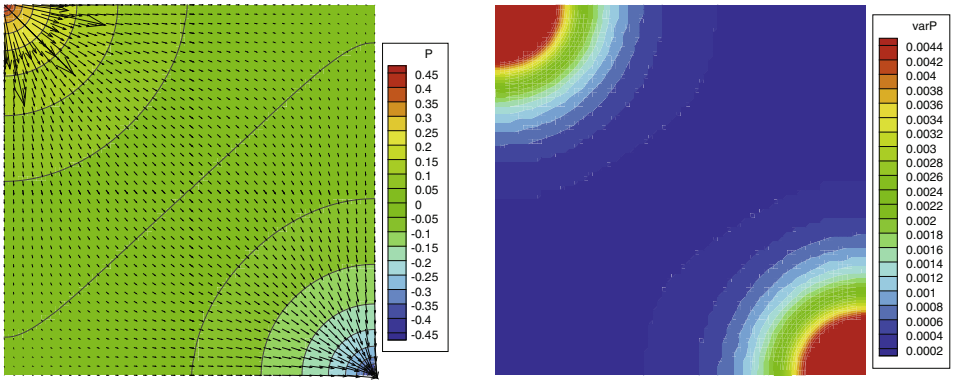

Fig. 4. Expectation of solution (left), and variance of the pressure (right) to problem B with 5^6 collocation points.

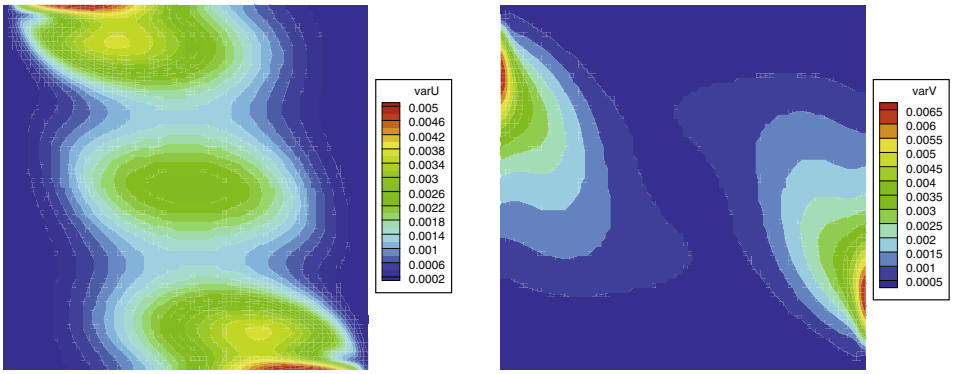

Fig. 5. Variance of the x-velocity component (left), and variance of the y-velocity component (right) to problem B with 5^6 collocation points.

Table 3
Stochastic convergence results for problem B

Coll. points	Flux L2 error	Pressure L2 error	Velocity L2 error
2^6	6.30703527E−05	6.41445607E−05	3.15266692E−05
3^6	2.39755565E−06	4.77299042E−07	1.14009004E−06
4^6	1.35972699E−07	3.45271568E−08	6.41590640E−08

7. Numerical results for slightly compressible flow

In this section, we model single phase slightly compressible flow using the IPARS framework [35,39,32]. To compare the stochastic collocation approaches with Monte Carlo, we consider a two dimensional reservoir 1280×1280 (ft^2) with a mean permeability field upscaled from the SPE10 Comparative Solution Upscaling Project data set as shown in Fig. 8.

The initial pressure is set at 3550 (psi). Injection wells are placed in each corner with a pressure of 3600 (psi), and a production well in placed in the center with a pressure of 3000 (psi). The numerical grid is 64×64 and the simulations run for 50 days with

Table 4
Stochastic convergence results for problem C

Coll. points	Flux L2 error	Pressure L2 error	Velocity L2 error
2^6	4.14095348E−02	1.63919311E−05	1.60948620E−02
3^6	5.04580970E−04	9.51941306E−07	2.58074051E−04
4^6	1.92383136E−05	1.25671461E−08	6.86101244E−06

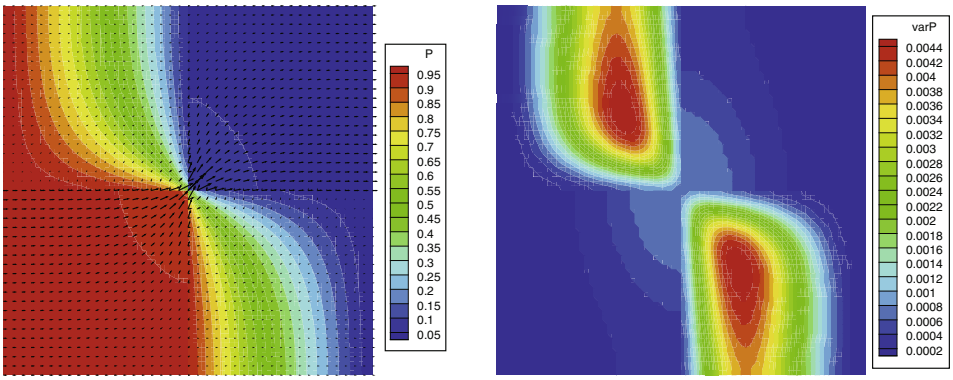

Fig. 6. Expectation of solution (left), and variance of the pressure (right) to problem C with 5^6 collocation points.

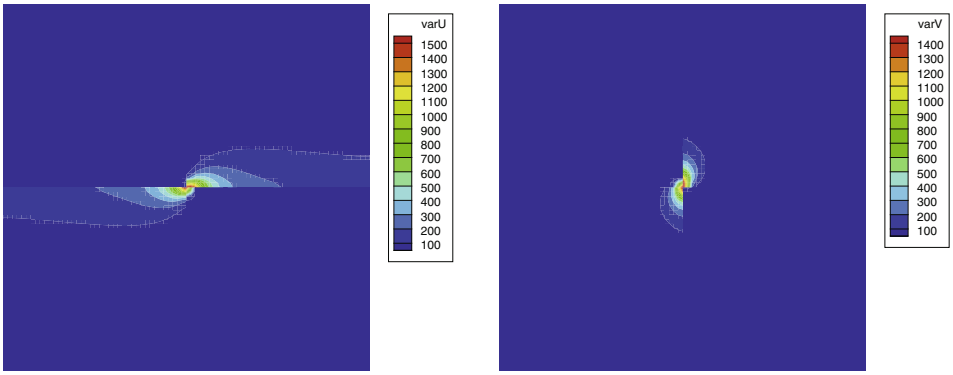

Fig. 7. Variance of the x-velocity component (left), and variance of the y-velocity component (right) to problem C with 5^6 collocation points.

Table 5
Deterministic convergence results for problem C

Grid	Flux L2 error	Pressure L2 error	Velocity L2 error
10×10	12.2307702	0.0116301201	5.50891085
20×20	12.7644499 (0.9582)	0.00879426323 (1.3225)	4.34814306 (1.2670)
40×40	11.9079145 (1.0719)	0.00573525999 (1.5334)	2.99591277 (1.4514)
80×80	8.28362644 (1.4375)	0.00274973298 (2.0858)	1.52456248 (1.9651)

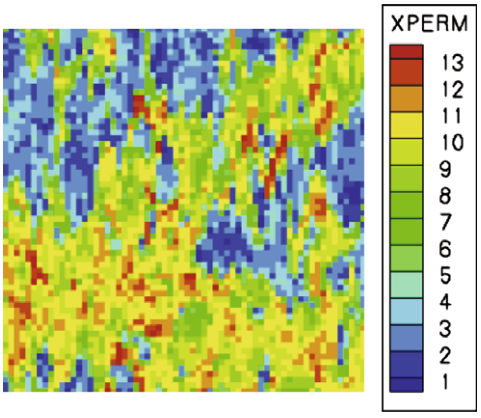

Fig. 8. Mean log-permeability field based on the SPE10 case.

variable time stepping. We assume $\sigma_Y = 1$ and a correlation length of 0.78 in each direction to enable the KL expansion to be truncated at four terms. The collocation points are taken to be tensor products of the roots of Hermite polynomials as described in Section 3.3.

In Fig. 9 we plot the mean pressure fields at $t = 50$ for the Monte Carlo and stochastic collocation simulations respectively. We include streamlines to indicate the direction of the flow. In Fig. 10 we plot the standard deviation of the pressure fields at $t = 50$ for the Monte Carlo and stochastic collocation simulations, respectively. In each case, we see that the stochastic collocation provides results comparable to the Monte Carlo while requiring fewer simulations. We note that the scale of the standard deviation of the pressure is significantly less than that of the mean.

Next, we compare some numerical results for two phase (oil and water) slightly compressible flow to the numerical results for single phase slightly compressible flow computed above. The mean permeability, the porosity, and the well models are same as the previous example. We also use the same Karhunen–Loeve expansion and collocation points. The initial oil pressure is set at 3550 [psi] and the initial water saturation is 0.2763.

In Figs. 11–13, we plot the mean and the standard deviation of the oil pressure, the water saturation, and the cumulative oil production respectively using 100 Monte Carlo simulations and 2^4 collocation points. The statistics computed using collocation are comparable to the Monte Carlo simulations while requiring less computational effort.

Comparing Figs. 9 and 11, we see that the mean and the standard deviation of the pressure fields have similar topological fea-

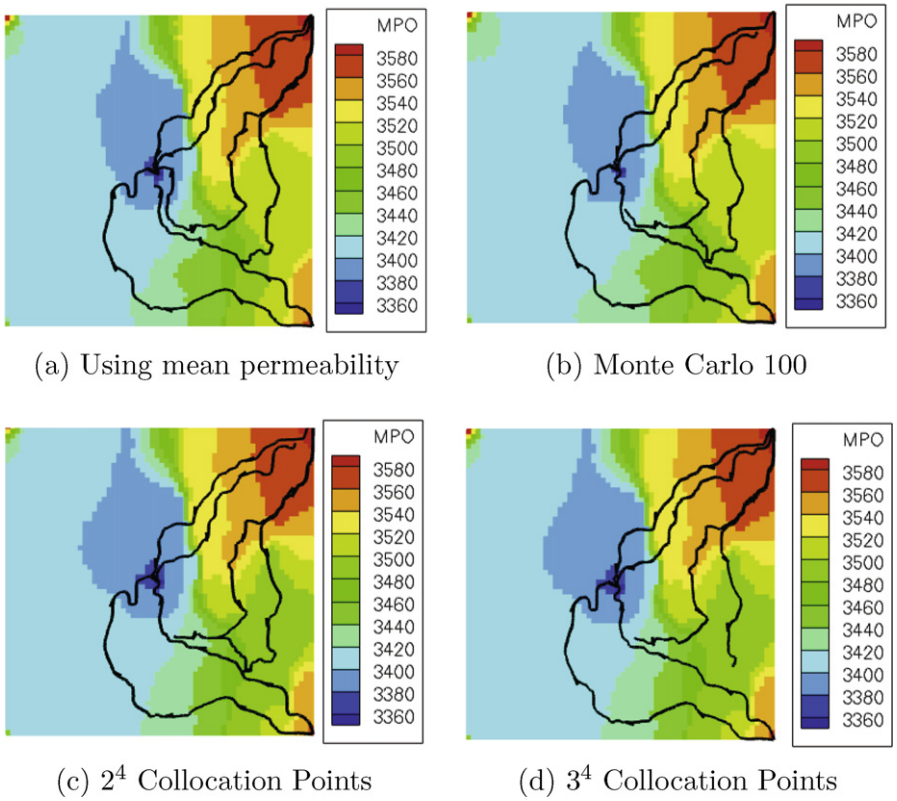

Fig. 9. Mean pressure field and streamlines for slightly compressible flow using the mean permeability (a), 100 Monte Carlo simulations (b), 2^4 collocation points (c), and 3^4 collocation points (d).

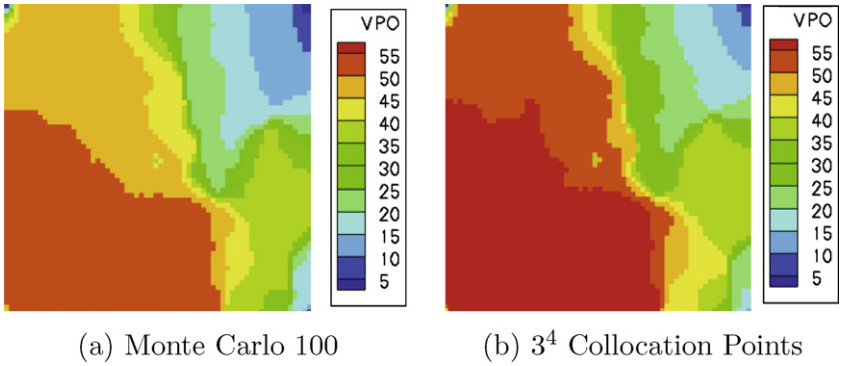

Fig. 10. Standard deviation of the pressure field for slightly compressible flow using 100 Monte Carlo simulations (a) and 3^4 collocation points (b).

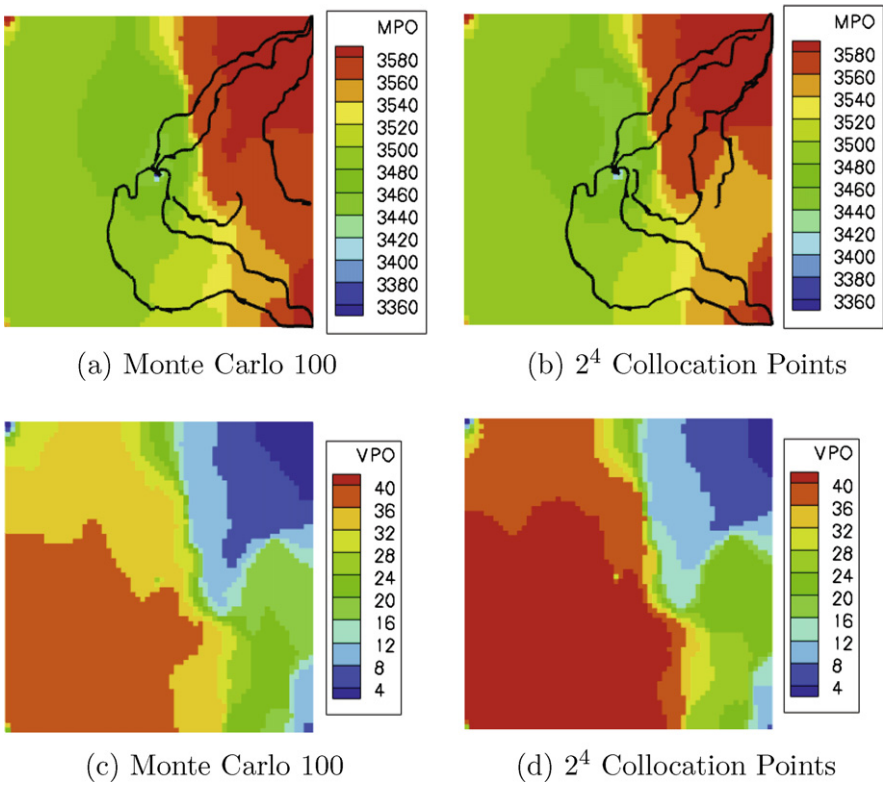

Fig. 11. Mean of the oil pressure and mean streamlines using 100 Monte Carlo simulations (a), the mean of the oil pressure and mean streamlines using 2^4 collocation points (b), the standard deviation of the oil pressure using 100 Monte Carlo simulations (c), and the standard deviation of the oil pressure using 2^4 collocation points (d).

tures. This indicates that we may be able to use the single phase solver, which is less expensive, to determine the appropriate number of terms in the Karhunen–Loeve expansion, to select the number of collocation points, or to design effective preconditioners.

To investigate the effect that changing σ_Y in (2.7) has on the output statistics, we repeat the above simulations for two phase flow with $\sigma_Y = 0.25$ and with $\sigma_Y = 3$. In each case we apply the collocation method with 3^4 points. In Figs. 14 and 15, we plot the mean and the standard deviation of the oil pressure respectively. Comparing with Fig. 11, we see that varying the standard deviation of the permeability field affects the scale of the uncertainty but not the overall topological features of the pressure field.

Finally, we compare the mean pressure field in Fig. 11 b with the mean pressure computed using different correlation lengths in the covariance function (2.7). In Fig. 16, we plot the mean pressure using $\eta_1 = 0.16$ and $\eta_2 = 0.23$ as well as the mean pressure using $\eta_1 = \eta_2 = 0.08$. We notice that the mean pressure differs only slightly in each case, despite using different correlation lengths. Theoretically, more terms in the KL expansion are required to accurately represent the output statistics for shorter correlation lengths. Current research is focusing on the development of *a priori* and *a posteriori* techniques to predict the sufficient number of terms in the KL expansion.

8. Conclusions

The present paper has focused on analyzing the combined use of stochastic collocation methods and mixed finite elements for quantifying the uncertainty of flow quantities for a given log-normal distributed permeability field. We have considered both incompressible and slightly compressible single phase flow as well as two-phase flow in a porous media. From a theoretical stand-

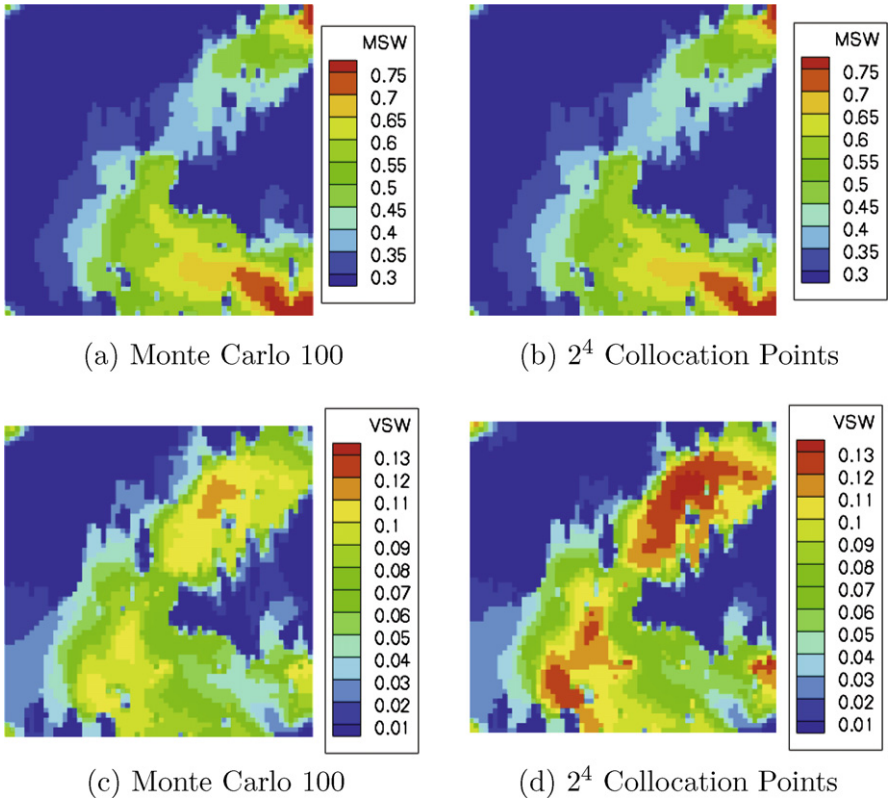

Fig. 12. Mean of the water saturation using 100 Monte Carlo simulations (a), the mean of the water saturation using 2^4 collocation points (b), the standard deviation of the water saturation using 100 Monte Carlo simulations (c), and the standard deviation of the water saturation using 2^4 collocation points (d).

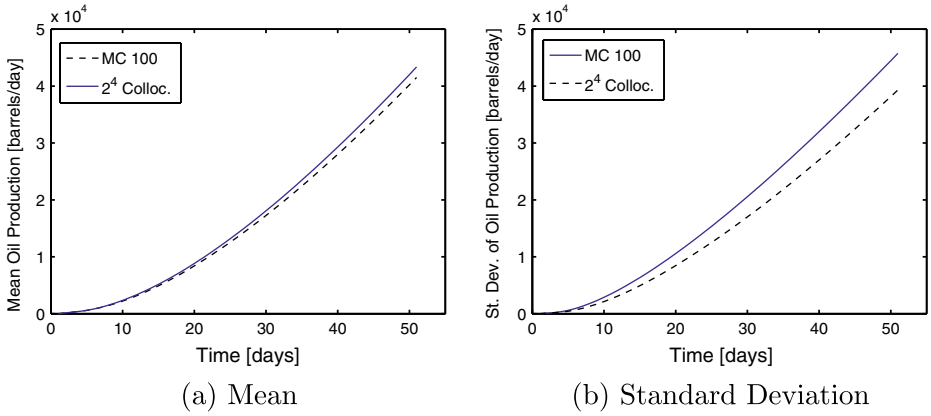

Fig. 13. Mean (a) and standard deviation (b) of the cumulative oil production using 100 Monte Carlo simulations and 2^4 collocation points.

point, we have established convergence bounds for both the pressure and the velocity. These results also hold for nonlinear diffusion coefficients as occurring in the event of slight compressibility.

From a numerical standpoint, we were able to confirm numerically the theoretical convergence rates for the stochastic and the deterministic errors. We also observed that the stochastic collocation converges much faster (to the mean and variance) than the standard MCS approach with a significantly reduced number of simulations. This observation also holds for the two-phase case where phase saturations follow a hyperbolic trend. The same stochastic numerical convergence was also verified for the well production curves.

The present work should set the basis for addressing a set of more challenging issues. These issues include: (1) extension of results on non-stationary distributions in a domain decomposition fashion (i.e., different subdomains following different random permeability distributions) to account for multiple permeability scales (some recent efforts on stochastic multiscale methods can be seen in [14,46]); (2) design of specialized solvers and time-stepping strategies capable of taking advantage of solution trends displayed by the closeness of multiple simulations; (3) experiences with probabilistic collocation methods and other stochastic interpolation methods seeking to reduce the computational burden due to the sampling and order of stochastic polynomial approximations; and (4) define the order of stochastic approximations for KL and Hermite polynomials for highly complex flow simulation models (e.g., compositional EOS flow) based on the stochastic of simpler flow models such as single-phase flow and streamlines, as well as incorporation of *a priori* information using Bayesian inference.

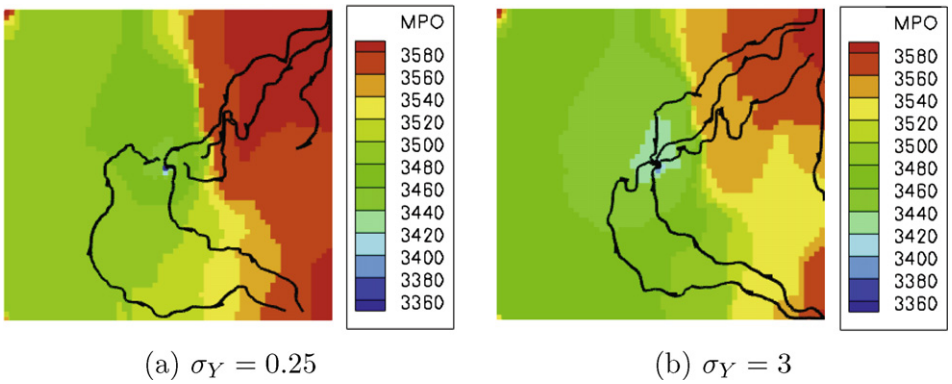

Fig. 14. Mean pressure field and streamlines using $\sigma_Y = 0.25$ (a) and using $\sigma_Y = 3$ (b) with 3^4 collocation points.

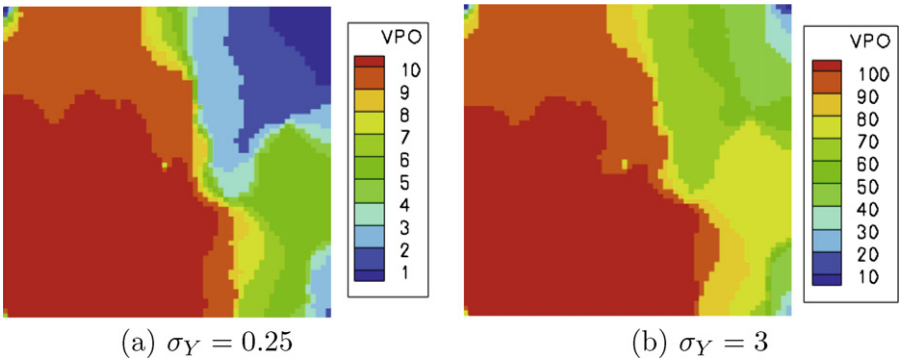

Fig. 15. Standard deviation of the pressure field using $\sigma_Y = 0.25$ (a) and using $\sigma_Y = 3$ (b) with 3^4 collocation points.

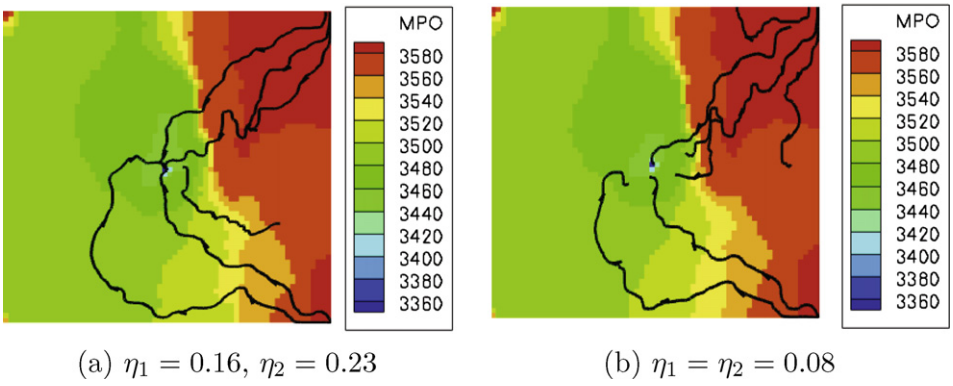

Fig. 16. Mean pressure field and streamlines using 3^4 collocation points with correlation length $\eta_1 = 0.16$ and $\eta_2 = 0.23$ (a), and $\eta_1 = \eta_2 = 0.08$ (b).

References

[1] M. Abramowitz, I.A. Stegun (Eds.), Handbook of Mathematical Functions with Formulas, Graphs, and Mathematical Tables, Chapter Orthogonal Polynomials (N. 22), Dover, 9th printing edition, 1972, pp. 771–802.
[2] I. Babuška, F. Nobile, R. Tempone, A stochastic collocation method for elliptic partial differential equations with random input data, SIAM J. Numer. Anal. 45 (3) (2007) 1005–1034. electronic.
[3] I. Babuska, R. Tempone, G.E. Zouraris, Galerkin finite element approximations of stochastic differential equations, SIAM J. Numer. Anal. 42 (2) (2004) 800–825.
[4] F. Brezzi, J. Douglas Jr., R. Duràn, M. Fortin, Mixed finite elements for second order elliptic problems in three variables, Numer. Math. 51 (1987) 237–250.
[5] F. Brezzi, J. Douglas Jr., M. Fortin, L.D. Marini, Efficient rectangular mixed finite elements in two and three space variables, RAIRO Modèl. Math. Anal. Numèr. 21 (1987) 581–604.
[6] F. Brezzi, J. Douglas Jr., L.D. Marini, Two families of mixed elements for second order elliptic problems, Numer. Math. 88 (1985) 217–235.
[7] F. Brezzi, M. Fortin, Mixed and hybrid finite element methods, Springer-Verlag, New York, 1991.
[8] M. Chen, D. Zhang, A. Keller, Z. Lu, Stochastic analysis of two phase flow in heterogeneous media by combining Karhunen–Loeve expansion and perturbation method, Water Resour. Res. 41 (1) (2005). W01006 (1–14).
[9] Z. Chen, J. Douglas Jr., Prismatic mixed finite elements for second order elliptic problems, Calcolo 26 (1989) 135–148.
[10] P.G. Ciarlet, The finite element method for elliptic problems, North-Holland, New York, 1978.
[11] L.C. Cowsar, C. Woodward, I. Yotov, PARCEL v1.04 user guide. Technical Report 96-28, TICAM, University of Texas at Austin, 1996.
[12] M.K. Deb, I.M. Babuška, J.T. Oden, Solution of stochastic partial differential equations using Galerkin finite element techniques, Comput. Methods Appl. Mech. Engrg. 190 (48) (2001) 6359–6372.
[13] G.S. Fishman, Monte Carlo: Concepts, Algorithms and Applications, Springer-Verlag, Berlin, 1996.
[14] B. Ganapathysubramanian, N. Zabaras, Modelling diffusion in random heterogeneous media: data-driven models, stochastic collocation and the variational multi-scale method, J. Comput. Phys. 226 (2007) 326–353.

[15] B. Ganapathysubramanian, N. Zabaras, Sparse grid collocation methods for stochastic natural convection problems, J. Comput. Phys. 225 (2007) 652–685.
[16] R.G. Ghanem, P.D. Spanos, Stochastic Finite Elements: A Spectral Approach, Springer-Verlag, New York, 1991.
[17] R. Ghanem, Scale of fluctuation and the propagation of uncertainty in random porous media, Water Res. 34 (2) (1998) 2123.
[18] T.Y. Hou, W. Luo, B. Rozovskii, H.-M. Zhou, Wiener chaos expansions and numerical solutions of randomly forced equations of fluid mechanics, J. Comput. Phys. 216 (2) (2006) 687–706.
[19] K.D. Jarman, T.F. Russell. Analysis of 1-D moment equations for immiscible flow, in: Fluid Flow and Transport in Porous Media: Mathematical and Numerical Treatment (South Hadley, MA, 2001), vol. 295 of Contemp. Math., Amer. Math. Soc., Providence, RI, 2002, pp. 293–304.
[20] K.D. Jarman, T.F. Russell, Eulerian moment equations for 2-D stochastic immiscible flow, Multiscale Model. Simul. 1 (4) (2003) 598–608. electronic.
[21] M. Kamiński, G.F. Carey. Stochastic perturbation-based finite element approach to fluid flow problems, Int. J. Numer. Meth. Heat Fluid Flow 15 (7) (2005) 671–697.
[22] M.-Y. Kim, F.A. Milner, E.-J. Park, Some observations on mixed methods for fully nonlinear parabolic problems in divergence form, Appl. Math. Lett. 9 (1) (1996) 75–81.
[23] M.-Y. Kim, E.-J. Park, S.G. Thomas, M.F. Wheeler, A multiscale mortar mixed finite element method for slightly compressible flows in porous media, J. Korean Math. Soc. 44 (2007) 1–17.
[24] D.P. Landau, K. Binder, A Guide to Monte Carlo Simulations in Statistical Physics, Cambridge University Press, UK, 2000.
[25] H. Li, D. Zhang, Probabilistic collocation method for flow in porous media: Comparisons with other stochastic methods, Water Resour. Res. 43 (2007) W09409, doi:10.1029/2006WR005673.
[26] Z. Lu, D. Zhang, A comparative study on quantifying uncertainty of flow in randomly heterogeneous media using Monte Carlo simulations, the conventional and KL-based moment-equation approaches, SIAM J. Sci. Comput. 26 (2) (2004) 558–577.
[27] Z. Lu, D. Zhang, Accurate efficient quantification of uncertainty for flow in heterogeneous reservoirs using the KLME approach, SPE J. 11 (2) (2006) 239–247.
[28] X. Ma, N. Zabaras, An adaptive hierarchical sparse grid collocation algorithm for the solution of stochastic differential equations, submitted for publication.
[29] J.C. Nedelec, Mixed finite elements in R^3, Numer. Math. 35 (1980) 315–341.
[30] F. Nobile, R. Tempone, C.G. Webster, A sparse grid stochastic collocation method for partial differential equations with random input data, Technical Report 85, Politecnico de Milano, Dept. di Matematica, MOX, SIAM J. Numer. Anal., submitted for publication.
[31] B. Oksendal, Stochastic Differential Equations: An Introduction with Applications, Springer-Verlag, Berlin, 1998.
[32] M. Parashar, J.A. Wheeler, J.C. Brown, G. Pope, K. Wang, P. Wang, A new generation EOS compositional reservoir simulator: Part II – framework and multiprocessing, 1997 SPE Reservoir Simulation Symposium, Houston, TX, 1997, SPE 37977.
[33] E.-J. Park, Mixed finite element methods for generalized Forchheimer flow in porous media, Numer. Meth. PDE 21 (2005) 213–228.
[34] D.W. Peaceman, Interpretation of well-block pressure in numerical reservoir simulation with non-square grid blocks and anisotropic permeability, Trans. AIME 275 (1983) 10–22.
[35] M. Peszynska, M.F. Wheeler, I. Yotov, Mortar upscaling for multiphase flow in porous media, Comput. Geosci. 6 (2002) 73–100.
[36] R.A. Raviart, J.M. Thomas, A mixed finite element method for 2nd order elliptic problems, in: Mathematical Aspects of the Finite Element Method, Lecture Notes in Mathematics, vol. 606, Springer-Verlag, New York, 1977, pp. 292–315.
[37] C. Schwab, R. Todor, Karhunen–Loève approximation of random fields by generalized fast multipole methods, J. Comput. Phys. 217 (2006) 100–122.
[38] R.A. Todor, C. Schwab, Convergence rates for sparse chaos approximations of elliptic problems with stochastic coefficients, IMA J. Numer. Anal. 27 (2007) 232–261.
[39] P. Wang, I. Yotov, M. Wheeler, T. Arbogast, C. Dawson, M. Parashar, K. Sephernoori, A new generation EOS compositional reservoir simulator: Part I – formulation and discretization, 1997 SPE Reservoir Simulation Symposium, Houston, TX, 1997, SPE 37979.
[40] X. Wan, G.E. Karniadakis, Beyond Weiner–Askey expansions: Handling arbitrary pdfs, J. Scient. Comput. 27 (1–3) (2006) 455–464.
[41] D. Xiu, J.S. Hesthaven, High-order collocation methods for differential equations with random inputs, SIAM J. Sci. Comput. 27 (3) (2005) 1118–1139. electronic.
[42] D. Xiu, G.E. Karniadakis, Modeling uncertainty in steady state diffusion problem via generalized polynomial chaos, Comput. Methods Appl. Mech. Eng. 191 (2002) 4927–4948.
[43] D. Xiu, D.M. Tartakovsky, A two-scale nonperturbative approach to uncertainty analysis of diffusion in random composites, Multiscale Model. Simul. 2 (4) (2004) 662–674. electronic.
[44] D. Xiu, D.M. Tartakovsky, Numerical methods for differential equations in random domains, SIAM J. Sci. Comput. 28 (3) (2006) 1167–1185. electronic.
[45] D. Xiu, Efficient collocational approach for parametric uncertainty analysis, Commun. Comput. Phys. 2 (2) (2007) 293–309.
[46] X.F. Xu, A multiscale stochastic finite element method on elliptic problems involving uncertainties, Comput. Methods Appl. Mech. Engrg. 196 (25–28) (2007) 2723–2736.
[47] D. Zhang, Z. Lu, An efficient high-order perturbation approach for flow in random porous media via Karhunen–Loève and polynomial expansions, J. Comput. Phys. 194 (2) (2004) 773–794.
[48] D. Zhang, Stochastic Methods for Flow in Porous Media: Coping with Uncertainties, Academic Press, San Diego, CA, 2002.